PROCEEDINGS OF SCIENCE

Glowing Axion Stars at Radio Frequencies

Günter Sigl,[a,*] **Dennis Maseizik**[a] **and Hyeonseok Seong**[b]

[a] *Universität Hamburg, II. Institute for Theoretical Physics, Luruper Chaussee 149, 22761 Hamburg, Germany*

[b] *Deutsches Elektronen-Synchrotron DESY, Notkestr. 85, 22607 Hamburg, Germany*

E-mail: guenter.sigl@desy.de, dennis.maseizik@desy.de, hyeonseok.seong@desy.de

Axion-like particles (ALPs) can be converted to photons either through the Primakoff effect in an external magnetic field or through a parametric resonance if ALPs constitute part of the dark matter and form a condensate in the form of so-called axion stars. For a given ALP-photon coupling and stable ALP star configurations, the occurrence of parametric resonance requires a minimal ALP star mass - the photon critical mass. ALP stars exceeding the photon critical mass can give rise to radio line emission if the ALP mass is in the micro-electron volt range. Here, we entertain the possibilty that ALP stars grow beyond this photon critical mass due to accretion from the surrounding galactic background of dark matter ALPs and estimate the resulting possible radio line signals from the galactic halo which strongly depends on the accretion model. Comparing with the observed radio background allows to put preliminary constraints on ALP-photon coupling and accretion scenario.

1st General Meeting and 1st Training School of the COST Action COSMIC WSIPers (COSMICWISPers)
5-14 September, 2023
Bari and Lecce, Italy

*Speaker

PoS(COSMICWISPers)026

1. ALP stars and parametric resonance

Axion-like particles (ALPs) can be described by a pseudo-scalar field a with a Lagrangian of the form

$$\mathcal{L}_a = \frac{1}{2}\partial_\mu a \partial^\mu a + \frac{g_{a\gamma\gamma}}{4}\, a\, F_{\mu\nu}\tilde{F}^{\mu\nu} - V_a(a)\,, \tag{1}$$

where $g_{a\gamma\gamma}$ describes ALP coupling to two photons, $F_{\mu\nu}$ and $\tilde{F}_{\mu\nu}$ are the electromagnetic field strength tensor and its dual, respectively, and $V_a(a)$ is the ALP potential which also contains a mass term of the form $m_a^2 a^2/2$ in addition to an ALP model dependent interaction potential that can often be neglected. Classical, stationary solutions of the resulting equations of motion including gravity describe condensates, sometimes also called solitons, which can form so-called ALP stars. If photons propagate in the background of such condensates, their amplitude can get parametrically enhanced. The local exponential growth rate can be estimated from the maximum growth rate of a homogeneous condensate as [1–4]

$$\mu \simeq g_{a\gamma\gamma} m_a a\,. \tag{2}$$

In an ALP star significant enhancement can occur if this rate is larger than the photon escape rate $\mu_{\rm esc} \simeq 1/(2R_*)$, where R_* is the radius of the ALP star, see also Ref. [5].

For typical ALP star configurations, as described, for example, in Ref. [4, 6] this can be translated into a lower limit on the ALP star mass, known as the photon critical mass,

$$M_{*,\gamma} \simeq 6.5\times 10^{-13} M_\odot \left(\frac{10^{-5}\,{\rm eV}}{m_a}\right)\left(\frac{10^{-11}{\rm GeV}^{-1}}{g_{a\gamma\gamma}}\right)^2\left(\frac{10^{11}{\rm GeV}}{f_a}\right)\left[\left(\frac{g_{a\gamma\gamma}f_a}{0.46}\right)^2 - \frac{1}{2}\right]^{1/2}\,, \tag{3}$$

where f_a is the Peccei-Quinn scale and a Gaussian profile was assumed for the wavefunction.

2. Modelling accretion on ALP stars

How ALP stars accrete ALPs from their surroundings is currently only understood at the qualitative level by means of numerical simulations [7], [8], [9]. We therefore consider three different scenarios, which are based on the observation that typically one ALP star forms in the center of so called miniclusters, or ALP haloes.

The first accretion scenario was investigated in the numerical simulations performed in Ref. [9], who employed a self-similar attractor model to explain the long-time growth of an isolated star-minicluster system. This model, which we refer to as *self-similar*, is based on the condensation of gravitationally interacting ALPs from the minicluster onto the ALP star.

In the other two accretion scenarios, the relation between the halo mass M_h and the ALP star mass M_* can be approximated as [10]

$$M_*(z) = M_{h,\rm min}(z)\left[\frac{M_h}{M_{h,\rm min}(z)}\right]^{1/3}\,, \tag{4}$$

where the redshift-dependent minimum halo mass is given by

$$M_{h,\rm min}(z) = 5\cdot 10^{-19} M_\odot\,(1+z)^{3/4}\left(\frac{m_a}{50\,\mu{\rm eV}}\right)^{-3/2}\,, \tag{5}$$

up to a factor of order unity. Once one estimates the accretion rate onto the minicluster of radius R_h this immediately provides the growth rate of the ALP star mass, assuming that the core-halo relation Eq. (4) is maintained due to virial equilibrium between core and halo. Assuming a spherically symmetric ALP dark matter distribution $\rho(R)$ in the Milky Way this results in the estimate

$$\frac{dM_*}{dt}(R) = \frac{1}{3}\left(\frac{M_h}{M_{h,\rm min}}\right)^{-2/3}\frac{dM_h}{dt}(R) = \frac{4\pi}{3}\left(\frac{M_h}{M_{h,\rm min}}\right)^{-2/3} R_h^2\,\rho(R)\,\langle v(R)\rangle_{\rm eff}\,, \tag{6}$$

at distance R from the galactic center, where

$$\langle v(R)\rangle_{\rm eff} \simeq \frac{v_{\rm esc}^2(M_h)}{v_{\rm vir}(R)} \tag{7}$$

is given by the escape velocity of the minicluster and the galactic virial velocity.

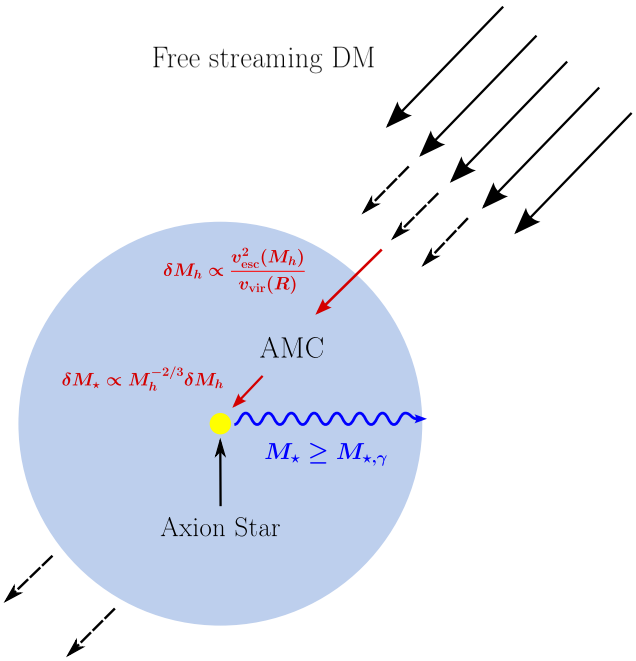

Figure 1: Minicluster accretion model for the core-halo system capturing background dark matter from the Milky Way dark matter halo in two stages: the ALP minicluster (AMC) in light blue captures the dark matter via gravitational interaction first, then the virialized axion star (yellow) accretes a part of the mass increase of the axion minicluster. [11]

Eq. (6) represents the *minimal accretion* scenario whereas Eq. (6) without the factor $(M_h/M_{h,\rm min})^{-2/3} < 1$ represents the *maximal accretion* scenario. These two scenarios are sketched in Fig. 1.

3. Estimates of radio line signatures from galactic ALP star accretion

We now assume that any ALP star satisfying $M_* \geq M_{*,\gamma}$ instantaneously radiates its accreted mass into monochromatic photons of energy $m_a/2$. Further assuming that roughly 70% of the galactic dark matter resides in ALP miniclusters and taking the minicluster mass distribution at

redshift $z = 0$ obtained from the linear Press-Schechter theory approach by [12], we can infer the total number and typical mass of galactic ALP miniclusters [11]. We translate the corresponding minicluster properties into an ALP star mass distribution via the core-halo relation Eq. (4) and integrate over the NFW-distributed ALP star population of the Milky Way, to predict the line strength of the resulting radio emission [11]. This will depend sensitively on the fraction of ALP stars with mass above the photon critical mass Eq. (3).

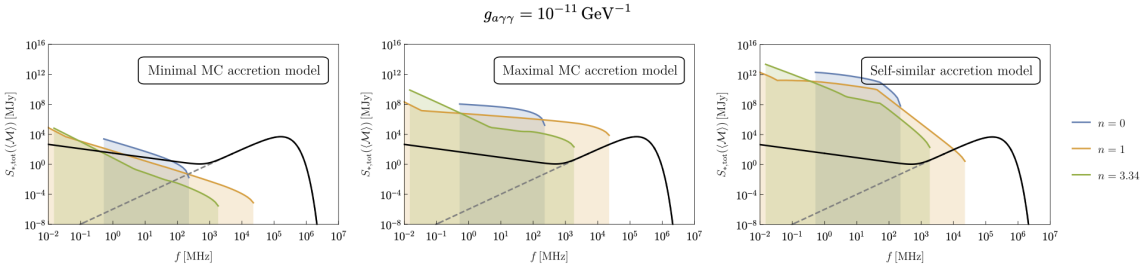

Figure 2: Total solid angle integrated radio line fluxes $S_{*,\mathrm{tot}}(m_a)$ from photon-critical axion stars in the Milky Way, predicted by the three accretion scenarios considered, for $g_{a\gamma\gamma} = 10^{-11}/\mathrm{GeV}$ as a function of the line frequency $f = m_a/(4\pi)$. The three coloured lines correspond to different effective ALP mass dependencies on temperature $m_a(T) = m_a[(m_a f_a)^{1/2}/T]^n$ for $T > (m_a f_a)^{1/2}$ in the early Universe, with n as indicated in the legend. The solid line is the solid angle integrated observed continuum radio background.

In Fig. 2 we show the resulting flux predictions compared to the observed radio background which consists of the cosmic microwave background and the astrophysical radio background at lower frequencies. Note that the predicted fluxes constitute narrow lines with a relative width given by the galactic virial velocity in terms of the speed of light at frequency $f = m_a/(4\pi)$, such that for a given ALP mass only the flux at that frequency is observable.

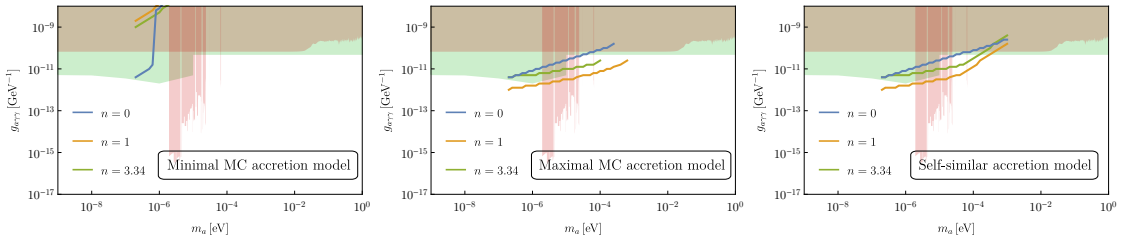

Figure 3: Preliminary exclusion plot for the coupling $g_{a\gamma\gamma}$ as a function of ALP mass m_a, based on requiring the predicted line fluxes shown in Fig. 2 to be smaller than the observed continuum radio background. As in Fig. 2 the three coloured lines correspond to different effective ALP mass dependencies on temperature in the early Universe. The horizontal color shades represent astrophysical constraints whereas the vertical shades show various experimental constraints.

In a first rough approximation, line fluxes above the observed fluxes are ruled out. This gives rise to the preliminary exclusion plots shown in Fig. 3. We note that a more detailed analysis, taking into account sensitivities of relevant radio telescopes and their capabilities to remove continuum fluxes will likely give rise to much stronger constraints. We will leave such investigations to future studies.

In summary, the predicted line fluxes inherit large uncertainties from the poorly understood ALP accretion mechanisms and from the linear-growth prediction of the galactic minicluster distribution

[12]. However, our preliminary results suggest that certain combinations of accretion scenario, ALP mass m_a and ALP-photon coupling $g_{a\gamma\gamma}$ can be strongly constrained by radio astronomy data.

Acknowledgements

We acknowledge support by the Deutsche Forschungsgemeinschaft (DFG, German Research Foundation) under Germany's Excellence Strategy – EXC 2121 "Quantum Universe" – 390833306. This article is based upon work from the COST Action COSMIC WISPers CA21106, supported by COST (European Cooperation in Science and Technology).

References

[1] M.P. Hertzberg and E.D. Schiappacasse, *Dark Matter Axion Clump Resonance of Photons*, *JCAP* **11** (2018) 004 [1805.00430].

[2] P. Carenza, A. Mirizzi and G. Sigl, *Dynamical evolution of axion condensates under stimulated decays into photons*, *Phys. Rev. D* **101** (2020) 103016 [1911.07838].

[3] D.G. Levkov, A.G. Panin and I.I. Tkachev, *Radio-emission of axion stars*, *Phys. Rev. D* **102** (2020) 023501 [2004.05179].

[4] M.P. Hertzberg, Y. Li and E.D. Schiappacasse, *Merger of Dark Matter Axion Clumps and Resonant Photon Emission*, *JCAP* **07** (2020) 067 [2005.02405].

[5] L.M. Chung-Jukko, E.A. Lim, D.J.E. Marsh, J.C. Aurrekoetxea, E. de Jong and B.-X. Ge, *Electromagnetic instability of compact axion stars*, *Phys. Rev. D* **108** (2023) L061302 [2302.10100].

[6] L. Visinelli, S. Baum, J. Redondo, K. Freese and F. Wilczek, *Dilute and dense axion stars*, *Phys. Lett. B* **777** (2018) 64 [1710.08910].

[7] B. Eggemeier and J.C. Niemeyer, *Formation and mass growth of axion stars in axion miniclusters*, *Physical Review D* **100** (2019) .

[8] J. Chen, X. Du, E.W. Lentz, D.J. Marsh and J.C. Niemeyer, *New insights into the formation and growth of boson stars in dark matter halos*, *Physical Review D* **104** (2021) .

[9] A.S. Dmitriev, D.G. Levkov, A.G. Panin and I.I. Tkachev, *Self-similar growth of Bose stars*, 2305.01005.

[10] H.-Y. Schive, M.-H. Liao, T.-P. Woo, S.-K. Wong, T. Chiueh, T. Broadhurst et al., *Understanding the core-halo relation of quantum wave dark matter from 3d simulations*, *Physical Review Letters* **113** (2014) .

[11] D. Maseizik, S. Mondal, H. Seong and G. Sigl, *Glowing Axion Stars: Accretion of Axion Dark Matter*, in preparation.

[12] M. Fairbairn, D.J. Marsh, J. Quevillon and S. Rozier, *Structure formation and microlensing with axion miniclusters*, *Physical Review D* **97** (2018) .